

NASA-CR-172,166

NASA Contractor Report 172166

ICASE

NASA-CR-172166
19830024070

PERTURBATION ANALYSIS OF THE LIMIT CYCLE
OF THE FREE VAN DER POL EQUATIONS

Mohammad B. Dadfar

James Geer

Carl M. Anderson

Contract No. NAS1-14101
June 1983

INSTITUTE FOR COMPUTER APPLICATIONS IN SCIENCE AND ENGINEERING
NASA Langley Research Center, Hampton, Virginia 23665

Operated by the Universities Space Research Association



NF02525

LIBRARY COPY

NASA

National Aeronautics and
Space Administration

Langley Research Center
Hampton, Virginia 23665

JUN 23 1983

LANGLEY RESEARCH CENTER
LIBRARY, NASA
HAMPTON, VIRGINIA

Perturbation Analysis of the Limit Cycle
of the Free van der Pol Equation #

Mohammad B. Dadfar
Department of Computer Science
Bowling Green State University
Bowling Green, Ohio 43404

James Geer*
Department of Systems Science
School of Advanced Technology
S.U.N.Y.
Binghamton, New York 13901

Carl M. Anderson**
Department of Mathematics
and Computer Science
College of William and Mary
Williamsburg, Virginia 23875

Abstract

A power series expansion in the damping parameter ϵ of the limit cycle $U(t; \epsilon)$ of the free van der Pol equation $\ddot{U} + \epsilon(U^2 - 1)\dot{U} + U = 0$ is constructed and analyzed. Coefficients in the expansion are computed up to $O(\epsilon^{24})$ in exact rational arithmetic using the symbolic manipulation system MACSYMA and up to $O(\epsilon^{163})$ using a FORTRAN program. The series is analyzed using Padé approximants. The convergence of the series for the maximum amplitude of the limit cycle is limited by two pair of complex conjugate singularities in the complex ϵ -plane. A new expansion parameter is introduced which maps these singularities to infinity and leads to a new expansion for the amplitude which converges for all real values of ϵ . Amplitudes computed from this transformed series agree very well with reported numerical and asymptotic results. For the limit cycle itself, convergence of the series expansion is limited by three pair of complex conjugate branch point singularities. Two pair remain fixed throughout the cycle, and correspond to the singularities found in the maximum amplitude series, while the third pair moves in the ϵ -plane as a function of t from one of the fixed pairs to the other. The limit cycle series is transformed using a new expansion parameter, which leads to a new series that converges for larger values of ϵ .

*Research supported in part by the National Aeronautics and Space Administration under NASA Contract No. NAS1-14101 while the author was in residence at the Institute for Computer Applications in Science and Engineering, NASA Langley Research Center, Hampton, VA 23665.

**Research supported by the NASA Langley Research Center, Hampton, Va 23665.

#Some of the computation for this work was performed on the MACSYMA symbolic manipulation system developed at the Laboratory for Computer Science, Massachusetts Institute of Technology, and supported in part by the National Aeronautics and Space Administration under Grant NSG 1323, by the United States Department of Energy under Grant ET-78-C-02-4687, by the Office of Naval Research under Grant N00014-77-C-0641, and by the U.S. Air Force under Grant F49620-79-C-020.

N83-32341#

1) Introduction

We wish to study the limit cycle $U(t;\epsilon)$ of the free van der Pol equation

$$(1.1) \quad \ddot{U} + \epsilon(U^2 - 1)\dot{U} + U = 0,$$

where the dots represent differentiation with respect to the independent variable t . We shall do this by constructing and analyzing the power series expansion of U in the damping parameter ϵ . We first wish to determine some of the analytical structure of U as a function of ϵ and, in particular, to determine the locations of the singularities of U in the complex ϵ -plane which are closest to the origin and, hence, limit the radius of convergence of the power series solution. Once the locations of these singularities have been determined, a new expansion of U can be constructed which will converge for larger values of ϵ .

This work is a companion paper to some work reported previously by Andersen and Geer [1] (henceforth referred to as I) on the power series expansions of the frequency and period of the limit cycle of the van der Pol equation. In I, the power series expansions of the frequency ν of the limit cycle U , as well as U itself, were computed up to a high number of terms. However, in I, only the series expansion of ν was analyzed in detail. In particular, it was found that the convergence of the series for ν was limited by a pair of complex conjugate branch point singularities in the complex ϵ^2 -plane. These branch points, which were located at $\epsilon^2 = \tilde{R} \pm i\tilde{\beta}$, with $\tilde{R} \approx 3.42$ and $\tilde{\beta} \approx 1.7925$, appear to be the only singularities of ν in

the finite part of the ϵ^2 -plane. Hence, when a new expansion parameter was introduced which mapped these singularities to infinity, the resulting expansion converged for all real values of ϵ . The values of the period computed from a completed form of this new expansion compared very well with reported numerical results, as well as with the asymptotic formula for the period valid for large values of ϵ .

In section 2 below, the problem of determining the limit cycle is formulated and the method we used to compute the power series expansions of v and U is described briefly. In section 3, the series for the maximum amplitude of U , corresponding to U at $t=0$, is analyzed using Padé approximants. It is found that the convergence of the series is limited by the presence of two pair of complex conjugate branch point singularities in the complex ϵ -plane, which correspond to the square roots of the singularities in the ϵ^2 -plane found for the frequency series. One pair of these singularities lies in the first and fourth quadrant, while the other pair lies in the second and third quadrant. A new expansion parameter is introduced in section 4 which leads to an expansion for the amplitude that converges for all real values of ϵ . Values of the amplitude computed from this series, and a modified version of it, are computed and found to compare very well with reported numerical results and also with values computed from the asymptotic formula for the amplitude valid for large ϵ .

The limit cycle itself is analyzed in section 5 using Padé approximants for values of t between 0 and T , where T is the period of the limit cycle. We now find that there are three pair of complex conjugate branch point singularities which lie about equidistant from the origin. For all values of t , two pair of these singularities remain fixed in the ϵ -plane at the same locations as the singularities for $t=0$ (i.e., for the amplitude series). At $t=0$, the location of the third pair of singularities coincides with the loca-

tion of the fixed singularities in the second and third quadrants. However, as t increases from zero, these singularities begin to move away from the fixed locations in the second and third quadrants toward the fixed locations in the first and fourth quadrants. In particular, they cross the imaginary axis in the complex ϵ -plane when $t=T/4$ and arrive at the fixed locations in the first and fourth quadrants at $t=T/2$. This motion of the singularities repeats itself for $T/2 \leq t \leq T$. Knowledge of the location of these singularities suggests a new expansion parameter and a transformation of the original series which will converge for larger values of ϵ . This is done in section 6, while our results are discussed in section 7.

2) Power Series Expansion in ϵ

We construct the power series expansion of the limit cycle of the free van der Pol equation (1.1) by first making the change of variables

$$(2.1) \quad x = vt,$$

where $v = v(\epsilon) = 2\pi/T(\epsilon)$ is the (unknown) frequency of the limit cycle and $T(\epsilon)$ is its (unknown) period. We then let

$$(2.2) \quad u(x;\epsilon) = U(t;\epsilon),$$

where u is now periodic in x with period 2π . In terms of u , equation (1.1) becomes

$$(2.3) \quad v^2 \ddot{u} + \epsilon v (u^2 - 1) \dot{u} + u = 0,$$

where the dots now denote differentiation with respect to x . In addition, we impose the phase condition that u have a maximum at $x=0$, i.e.,

$$(2.4) \quad \dot{u}(0,\epsilon) = 0, \quad u(0,\epsilon) = A(\epsilon) > 0.$$

We now look for solutions for $v(\epsilon)$, $u(x;\epsilon)$, and $A(\epsilon)$ in the form

$$(2.5) \quad v(\epsilon) = 1 + \sum_{j=1}^{\infty} v_j \epsilon^j,$$

$$(2.6) \quad u(x;\epsilon) = \sum_{j=0}^{\infty} u_j(x) \epsilon^j,$$

$$(2.7) \quad A(\epsilon) = \sum_{j=0}^{\infty} a_j \epsilon^j.$$

Here, each v_j and a_j is an unknown constant, while the unknown functions $u_j(x)$ must be periodic with period 2π . Substituting (2.5) and (2.6) into (2.3) and then (2.6) and (2.7) into (2.4), we are led to a sequence of linear problems from which the u_j can be determined recursively. In particular, demanding that each of the u_j is periodic in x leads to the unique determination of the constants v_j and a_j (see I, section 2, for details). In this way we find

$$v_{2i+1} = a_{2i+1} = 0, \quad i = 0, 1, 2, \dots,$$

while the $u_j(x)$ have the form

$$u_{2i} = \sum_{k=0}^{2i} u_{2i,k} \cos((2k+1)x),$$

$$u_{2i+1} = \sum_{k=0}^{2i+1} u_{2i+1,k} \sin((2k+1)x), \quad i = 0, 1, 2, \dots,$$

where the $u_{j,k}$ are certain constants.

Through the use of the symbolic manipulation system MACSYMA we have determined the coefficients in the expansions of both $v(\epsilon)$ and $u(x, \epsilon)$ up to $O(\epsilon^{24})$ in exact rational arithmetic. The exact rational expressions for the coefficients v_j are reported in I, while the first few terms in the expansions of $A(\epsilon)$ and u are

$$(2.8) \quad A = 2 + \frac{1}{96}\epsilon^2 - \frac{1033}{552960}\epsilon^4 + \frac{1019689}{55738368000}\epsilon^6 \\ + \frac{9835512276689}{157315969843200000}\epsilon^8 \\ - \frac{58533181813182818069}{7326141789209886720000000}\epsilon^{10} + O(\epsilon^{12}),$$

$$(2.9) \quad u = 2\cos x + \left(\frac{3}{4}\sin x - \frac{1}{4}\sin 3x\right)\epsilon + \left(-\frac{1}{8}\cos x + \frac{3}{16}\cos 3x - \frac{5}{96}\cos 5x\right)\epsilon^2 \\ + \left(-\frac{7}{256}\sin x + \frac{21}{256}\sin 3x - \frac{35}{576}\sin 5x + \frac{7}{576}\sin 7x\right)\epsilon^3 \\ + \left(\frac{73}{12288}\cos x - \frac{47}{1536}\cos 3x + \frac{1085}{27648}\cos 5x - \frac{2149}{110592}\cos 7x + \frac{61}{20480}\cos 9x\right)\epsilon^4 \\ + O(\epsilon^5).$$

We then constructed a FORTRAN program (using floating-point arithmetic) which evaluated the various coefficients up to terms which are $O(\epsilon^{163})$. (See I, section 2, for some details which expedited the computations.) In particular the coefficients a_0, a_2, \dots, a_{98} computed from this program are listed in floating point form in Table I.

Using some of the same ideas as in I for the frequency series, we now wish to investigate the convergence of the series (2.6) and (2.7). In particular, we wish to determine the location of the singularities of $u(x, \epsilon)$ in the complex ϵ -plane which are closest to the origin, and, hence, which limit the convergence of these series.

3) Analysis of the Amplitude Series

We begin our analysis of the limit cycle by considering the series for the maximum amplitude $A(\epsilon)$. Using the phase condition (2.4), it follows that

$A(\epsilon) = u(0; \epsilon)$, or

$$(3.1) \quad A(\epsilon) = \sum_{j=0}^{\infty} a_{2j} \epsilon^{2j}, \text{ where } a_{2j} = u_{2j}(0).$$

Values of $A(\epsilon)$ determined by (3.1) for ϵ between 0 and about 2 are indicated by the dotted line in Fig. 1. Clearly, the series diverges for ϵ close to 2. The root test on the coefficients a_{2j} provides the estimate that the radius of convergence R_0 of the series (3.1) is approximately 1.86.

In order to investigate the convergence of the amplitude series more closely, a sequence of $[N/N]$ Padé approximants were constructed from the Taylor series expansion (3.1) for $N = 20, 24, 28, \dots, 64$. The location of the zeros and poles of the approximants in the complex ϵ -plane were determined for each value of N . Since $A(\epsilon)$ is a real function of ϵ , any of the zeros or poles which did not lie on the real axis had to appear in complex conjugate pairs. In Fig. 2, we have shown the location of the zeros and poles for the $[48/48]$ Padé

approximant which lie in the upper half ϵ -plane. The pattern of nearly overlapping zeros and poles in Fig. 2 is similar to the pattern observed in the analysis of the series for $v(\epsilon)$ in I and indicates the presence of two pair of branch point singularities located at

$$(3.2) \quad \epsilon = \pm R_0 e^{\pm i\beta_0}, \quad R_0 \cong 1.85, \quad \tilde{\beta}_0 \cong 0.8770.$$

Thus, we see that the convergence of the series (3.1) is limited by the presence of two pair of complex conjugate singularities located (approximately) at the points indicated by (3.2). These singularities also provide an estimate of the radius of convergence R_0 , which is consistent with the estimate obtained from the root test. We note that these singularities are very close to (most probably equal to) the singularities found in the series expansion of $v(\epsilon)$ in I. (In I, the singularities of $v(\epsilon)$ were found in the form $\epsilon^2 = \tilde{R} e^{\pm i\tilde{\beta}}$, or $\epsilon = \pm \tilde{R}^{1/2} e^{\pm i\tilde{\beta}/2}$, with $\tilde{R}^{1/2} \cong (3.42)^{1/2} \cong 1.849$ and $\tilde{\beta}/2 \cong 1.7925/2 = 0.89625$. These values are close to those given in (3.2).) In Fig. 1, we have indicated by the solid line the amplitude predicted by the [48/48] Padé approximant for values of ϵ between 0 and 9. We note that the Padé approximant agrees well with the series (3.1), where it converges, and also agrees well with some values for the amplitude computed by purely numerical methods. (These numerical methods will be discussed in more detail in the next section).

4) Transformation of the Amplitude Series

We can now use the information obtained in the previous section to introduce a new expansion parameter which will lead to a new series representation for $A(\epsilon)$, which will converge for larger values of ϵ . To do this, we introduce a new expansion parameter $\delta = \delta(\epsilon)$, defined by the transformation

$$(4.1) \quad \delta(\epsilon) = \frac{\epsilon}{\{R_0^4 - 2R_0^2 \epsilon^2 \cos 2\beta_0 + \epsilon^4\}^{1/4}}$$

where R_0 and β_0 are given (approximately) by (3.2). The transformation (4.1)

has the properties that the origin remains fixed (i.e., $\delta(0) = 0$), the singularities $\pm R_0 e^{\pm i\beta_0}$ in the ϵ -plane are mapped to infinity in the complex δ -plane (i.e., $|\delta(\pm R_0 e^{\pm i\beta_0})| = \infty$), and the real axis in the ϵ -plane is mapped onto the portion of the real axis in the δ -plane between -1 and +1 (in particular, as $\epsilon \rightarrow +\infty$, $\delta \rightarrow +1^-$). In addition, it is a simple task to invert the transformation (4.1) to express ϵ as a function of δ .

Using the definition (4.1), we recast the series (3.1) for $A(\epsilon)$ into a series in powers of δ of the form

$$(4.2) \quad A(\epsilon) = \sum_{j=0}^{\infty} a_{2j} \epsilon^{2j} = \sum_{j=0}^{\infty} \tilde{a}_{2j} \delta^{2j}$$

where the new coefficients \tilde{a}_{2j} can be expressed in terms of the coefficients a_{2j} and the transformation (4.1) in a straightforward manner. Since the singularities at $\pm R_0 e^{\pm i\beta_0}$ appear to be the only singularities of $A(\epsilon)$ in the finite part of the ϵ -plane, we expect that the series (4.2) will converge for all values of δ with $|\delta| < 1$. On the other hand, since $A(\epsilon)$ has an essential singularity at ϵ equal to infinity (see [2], for example), we would not expect the series (4.2) to converge for values of δ with $|\delta| > 1$.

To investigate this point quantitatively, we performed a Padé analysis on the series (4.2) using the coefficients \tilde{a}_{2j} . The zeros and poles of the Padé approximants again formed patterns indicating branch point singularities (in the complex ϵ -plane), this time lying on the real and imaginary axes at distances from the origin slightly greater than one. (For example, for the [48/48] approximant, the closest zero-pole pair was on the imaginary axis at a distance of 1.015 from the origin.) Thus, it appears that the radius of convergence for the series $A(\delta)$ is nearly one. The root test on the coefficients \tilde{a}_{2j} gives a result consistent with the value of one. We have used the series (4.2) to compute values of A for selected values of ϵ between 1 and 100, which correspond to values of δ for which good numerical results

are available (see, e.g., Zonneveld [7]). The results are presented in the third and fourth columns of Table II and show that the series (4.2) agrees well with the numerical results, with a maximum error of about 0.79% at $\epsilon = 100$. In Figure 3, we have plotted $A(\delta)$ using (4.2) (dotted line) for δ close to one. Note that the vertical scale in Fig. 3 is $100(A-2)$, and, hence, the agreement between $A(\delta)$ and the numerical results is better than might be indicated at first glance.

We can now use some information about the asymptotic behavior of the amplitude as $\epsilon \rightarrow \infty$ to improve the convergence of our series for $A(\delta)$ near $\delta = 1$ (i.e., for large values of ϵ). As $\epsilon \rightarrow \infty$, we know (see [5], for example) that

$$(4.3) \quad A = 2 - \frac{\alpha}{3}\epsilon^{-4/3} - \frac{16}{27} \frac{\log \epsilon}{\epsilon^2} + \frac{1}{9}(3\beta-1 + 2\log 2 - 8\log 3)\epsilon^{-2} + O(\epsilon^{-8/3}),$$

where $\alpha \cong -2.3381$ is the highest zero of the Airy function and $\beta \cong 0.1723$.

Since $\delta = 1 + C\epsilon^{-2} + O(\epsilon^{-4})$, as $\epsilon \rightarrow \infty$, the form of (4.3) suggests that we write $A(\delta)$ as

$$(4.4) \quad A(\delta) = 2 + (1-\delta^2)^{2/3} \sum_{j=0}^{\infty} b_{2j} \delta^{2j},$$

where the constants b_{2j} can be determined from the coefficients \tilde{a}_{2j} . We note that the representation (4.4) has the properties that $A = 2$ when $\delta = 0$ or $\delta = 1$ (i.e., when $\epsilon = 0$ or $\epsilon = \infty$) and also that, as $\delta \rightarrow 1$, or $\epsilon \rightarrow \infty$, the asymptotic form of (4.4) agrees with the form of the first two terms in (4.3).

Amplitudes computed from (4.4) are listed in the fifth column of Table II for values of ϵ between 1 and 100. We see that, for values of ϵ greater than 8, the series (4.4) agrees more closely with the numerical results than does the series (4.2). In Table III we have compared values of the amplitude computed from the series (4.2) and (4.4) with the four term asymptotic formula (4.3) for $A(\epsilon)$. The differences between the amplitudes computed from (4.2) and the asymptotic formula (4.3) steadily increase as ϵ increases, approaching a maximum error of about 0.85% at infinity. However, when (4.4) is used,

these differences steadily decrease, the agreement being perfect (by design) at $\delta = 1$ (i.e., infinite ϵ). In Figure 3, we have also plotted the values of $100(A-2)$ using (4.4). Again, the close agreement as $\delta \rightarrow 1$ among the values for the amplitude computed from (4.4), (4.3), and the numerical results can be clearly seen.

5) Analysis of the Limit Cycle Series

We now investigate the convergence of the limit cycle series (2.6) for values of x between 0 and π . (Since each $u_k(x+\pi) = -u_k(x)$ for all x , the behavior of the convergence of the series for x between π and 2π will be the same as the behavior for x between 0 and π). In Figure 4, we show the phase plane plots of the limit cycle, using the first 100 terms in (2.6) for $\epsilon = 0, 1.0, 1.5,$ and 1.6 . The plots for $\epsilon = 1.0$ and 1.5 are smooth and agree very well with similar plots computed by purely numerical means. However, for $\epsilon = 1.6$, we notice that, while most of the cycle is smooth and, in fact, agrees very well with the true cycle, portions of the curve in the second and fourth quadrant have developed oscillations which are not present in the actual limit cycle. These oscillations become more pronounced as ϵ is slowly increased above 1.6, although certain portions of the curve still remain smooth. For $\epsilon = 1.8$, however, the limit cycle computed from (2.6) is completely meaningless.

The non-uniform behavior of the convergence of the series representation of the limit cycle suggests that its radius of convergence may vary with x . In particular, the portions of the phase plane plots where the (artificial) oscillations appear correspond to values of x near $\pi/2$ and $3\pi/2$. This suggests that the radius of convergence of (2.6) may be somewhat smaller for values of x near $\pi/2$ and $3\pi/2$ than for other values of x .

In order to investigate this behavior more carefully, we performed a Padé analysis on the coefficients $u_j(x)$ for values of x between 0 and π , in increments

of $\pi/50$. For values of x between 0 and about $\pi/4$, the analysis indicated the presence of only the same two pair of complex conjugate branch points which were present for the amplitude series, i.e., for $x = 0$ (see Figure 2). In Figure 5, (a) and (b), we show the location of the zeros and poles of the $[24/24]$ Padé approximant which lie in the upper half complex plane for $x = \pi/50$ and $x = 13\pi/50$. As x was increased to values greater than $\pi/4$, however, something quite different and very interesting happened. It appears that, as x increases above $\pi/4$, a "new" singularity leaves its position in the second quadrant and moves toward the imaginary axis. In Figures 5 (c) and (d) we show the zeros and poles of the $[24/24]$ Padé approximant for $x = 18\pi/50$ and $x = 24\pi/50$, which clearly indicate the presence of this "moving singularity", while also indicating that there is still a singularity which remains fixed in the second quadrant. At $x = \pi/2$, the moving singularity crosses the imaginary axis. As x increases above $\pi/2$, the moving singularity enters the first quadrant, and moves toward the position of the "fixed singularity" in that quadrant. At about $x = 3\pi/4$, it appears to coalesce (at least approximately) with the fixed singularity and remains there for x between $3\pi/4$ and π . As x varies between π and 2π , the phenomena described above exactly repeats itself, with a singularity again moving from the second to the first quadrant. Of course, a similar phenomenon is happening simultaneously in the lower half plane.

Thus, it appears that the limit cycle series (2.6) has three pairs of complex conjugate singularities in the complex ϵ -plane, two pairs remaining fixed as x varies, while the third pair moves as a function of x . We have illustrated this schematically in Figure 6, indicating in the upper half complex ϵ -plane the location of the fixed singularities and also the approximate location of the moving singularity for various values of x .

From a knowledge of the location of these singularities, we can estimate

the radius of convergence R of the series (2.6). In particular, the radius of convergence will be just the distance from the origin to the closest singularity. For $0 \leq x \leq \pi/4$ and $\frac{3\pi}{4} \leq x \leq \pi$, when the moving singularity coincides (at least approximately) with the fixed singularities, the Padé analysis gives $R \cong 1.85$. However, for $\pi/4 < x < 3\pi/4$, the moving singularity becomes the dominant singularity, moving closer to the origin than the fixed singularities. Thus, R decreases for $\pi/4 \leq x \leq \pi/2$, reaching a minimum of about 1.65 at $x = \pi/2$, and then increases to about 1.85 at $x = 3\pi/4$. (We compared the values for R we obtained from the Padé analysis with values of R computed using the root test and found the results to be consistent.) We have plotted R as a function of x in Figure 7 (a). As mentioned earlier, the smaller radius of convergence of the series (2.6) for x near $\pi/2$ accounts for the presence of the oscillations in certain portions of the phase plane plots in Figure 4. In particular, for $\epsilon = 1.6$ (Figure 4 (d)), the oscillations occur for values of x near $\pi/2$ (and $3\pi/2$), indicating that this value of ϵ is close to the radius of convergence in this region. However, for x not near $\pi/2$ or $3\pi/2$, $\epsilon = 1.6$ is far enough from the radius of convergence to render the first 100 terms in (2.6) (used to calculate the plots in Figure 4) a good approximation to the true solution.

In Figure 7 (b) we have plotted the angle β as a function of x . Here β is the angle which the moving singularity makes with the positive real axis. Although we have not been able to determine with any great certainty what the moving singularity is "doing" for $0 \leq x \leq \pi/4$, there is some evidence that it may possibly be spiraling out from its location at $x = 0$. One piece of evidence to support this conjecture is the little "bump" in Figure 7 (b) near $x = \pi/4$, as well as smaller oscillations for $x < \pi/4$ which are too small to show up on the figure. Similar, but less pronounced, oscillations occur near $x = \pi/4$ in the plot of $R(x)$. Of course, similar oscillations occur near $x = 3\pi/4$,

indicating that the singularity may spiral into its location at $x = \pi$ in the first quadrant. However, since we are dealing with very small oscillations and since we have two pairs of singularities coalescing, our numerical results are not accurate or stable enough to make any definite statement about this conjecture.

6) Transformation of the Limit Cycle Series

Using our knowledge of the location of singularities of the limit cycle in the complex ϵ -plane, it is possible to introduce a new expansion parameter which will allow us to recast the original series (2.6) into a form which will converge for larger values of ϵ . To do this, we let $\epsilon = \pm R_0 e^{\pm i\beta_0}$ be the locations of the fixed singularities and $\epsilon = R e^{\pm i\beta}$ be the locations of the moving singularities. Here $R_0 \cong 1.85$ and $\beta_0 \cong 0.8970$, while R and β are functions of x , as indicated in Figure 7. If we now define

$$(6.1) \quad w = w(\epsilon) \frac{\epsilon}{\{(R_0^4 - 2R_0^2 \cos 2\beta_0 \epsilon^2 + \epsilon^4)(R^2 - 2R \cos \beta + \epsilon^2)\}^{1/6}},$$

we see that $w(0) = 0$, $|w| \rightarrow 1$ as $|\epsilon| \rightarrow \infty$, and $|w| \rightarrow \infty$ as ϵ approaches any one of the six singularities of u . Using (6.1) we can recast (2.6) into the form

$$(6.2) \quad u(x; \epsilon) = \sum_{j=0}^{\infty} u_j(x) \epsilon^j = \sum_{j=0}^{\infty} \tilde{u}_j(x) w^j,$$

where the functions \tilde{u}_j can be determined in a straightforward manner. We performed a root test on the coefficients \tilde{u}_j for values of x between 0 and π and found in each case an estimated radius of convergence very close to one. We also performed a Padé analysis of the coefficients \tilde{u}_j and found again a constant radius of convergence very close to one. In particular, for each value of x , the Padé analysis indicated singularities of u in the

complex w -plane very near $w = \pm 1$. These singularities are related, of course, to the essential singularity of u at ϵ equal to infinity.

To obtain some phase plane plots using the transformed series (6.2), we found it more convenient to use a transformation which is simpler (but less accurate) than (6.1). (For practical computations, the use of (6.1) requires the recomputation of the series coefficients \tilde{u}_j for each value of x used, since R and β , and hence $w(\epsilon)$, depend on x .) Instead of (6.1), we used the transformation

$$(6.3) \quad \tilde{w} = \tilde{w}(\epsilon) = \frac{\epsilon}{\{(R_0^4 - 2R_0^2 \cos 2\beta_0 \epsilon^2 + \epsilon^4)(R_m^2 + \epsilon^2)\}^{1/6}}$$

where $R_m = \min R(x) \cong 1.65$. Here \tilde{w} has the same mapping properties as w , except that it maps the moving singularity to infinity only when it is closest to the origin, i.e., when $x = \pi/2$. Thus, the region in the ϵ -plane containing the singularities is mapped out away from the origin, but not all the way to infinity. The advantage of (6.3), of course, is that it is independent of x and needs to be inverted only once during the computations to express ϵ as a function of \tilde{w} .

Using (6.3), we recast the series (2.6) into a form similar to (6.2), with w replaced by \tilde{w} . A Padé analysis of this transformed series revealed that it has a minimum radius of convergence of about 0.953, which corresponds to a radius of convergence in the ϵ -plane of about 3.97. In Figure 8, we show the phase plane plots of u using this transformed series for $\epsilon = 1.65$ and $\epsilon = 3.5$.

7) Discussion

The method of analysis we have presented here is an interesting combination of the methods of regular perturbation analysis and classical analysis, with both symbolic and numerical computation used to carry out the details of the

methods. As we mentioned in I, the importance of the role of symbolic computations in this analysis should not be underestimated. Among other advantages, it allowed us to find certain patterns and forms of the solutions which greatly facilitated the construction of an efficient numerical FORTRAN program to carry the computations further. Also, the coefficients in the various expansions obtained by symbolic computation, being in exact rational number form, allowed us not only to check the results of our FORTRAN program but also to estimate the magnitude and effects of roundoff errors in our numerical computations.

As far as the practical application of our results is concerned, it is interesting to note that we have been able to present formulas for the frequency and limit cycle function, valid for large values of ϵ , by knowing only the approximate locations of the singularities of the functions involved. In particular, we have obtained our results without having to investigate the nature (or type) of the singularities that occur (e.g., we have not had to determine whether we have an algebraic or logarithmic singularity or a singularity of some other kind). In this sense, the methods we have used are quite powerful, especially in that all we really needed to know to make them work was a knowledge of the approximate location of the singularities, and not their exact location. It is interesting to point out, however, that the location of the singularities for this problem, being off the real axis, is in sharp contrast to the location of the singularities for "most" other physical problems which have been analyzed by similar methods (see e.g., Van Dyke [6]).

As far as the nature of the singularities is concerned, however, we have applied the method of analysis given by Hunter and Guerrieri [3] to the frequency series we developed in I and to the maximum amplitude series $u(0;\epsilon)$, discussed in sections 3 and 4, which were both essentially series in powers of ϵ^2 . The result of this analysis indicated that the singularities in

these cases are algebraic singularities with an exponent of $\frac{1}{2}$, i.e., square root singularities. However, the method of [3] does not work well when more than one pair of complex conjugate singularities are about at equal distance from the origin, as in the case of the series (2.6) for $x > 0$, and hence we have no definite knowledge of the nature of the singularities for u when $x > 0$.

References

- [1] C.M. Andersen and J.F. Geer, "Power series expansions for the frequency and period of the limit cycle of the Van der Pol equation", S.I.A.M. J. Appl. Math., 42 (1982), pp. 678-693.
- [2] A.A. Dorodnicyn, "Asymptotic Solution of Van der Pol's Equation," Priklad. Math i Mekh II (1947) 313-328 (in Russian), Amer. Math. Soc. Transl. No. 88 (1958) (English version).
- [3] C. Hunter and B. Guerrieri, "Deducing the Properties of Singularities of Functions from Their Taylor Series Coefficients," SIAM J. Appl. Math. Vol. 39 (1980) pp. 248-263.
- [4] MACSYMA Reference Manual, The Mathlab Group, Version Nine, Laboratory for Computer Science, Mass. Institute of Technology, Cambridge, Ma., 1977.
- [5] P.J. Ponzio and N. Wax, "On the periodic solution of the Van der Pol Equation," IEEE Trans. Circuit Theory, CT-12 (1965), pp. 135-136.
- [6] M. VanDyke, "Analysis and improvement of perturbation series," Q.J. Mech. Appl. Math., 27 (1974), pp. 423-450.
- [7] J.A. Zonnerveld, "Periodic solutions of the Van der Pol Equation," Indag. Math., 28 (1966), pp. 620-622.

Figure Captions

<u>Figure</u>	<u>Caption</u>
1	Maximum amplitudes $A(\epsilon)$ of the limit cycle calculated from (3.1) (dotted line) and the [48/48] Padé approximant (solid line) for $0 \leq \epsilon \leq 9$. The heavy dots are the values of amplitude computed using purely numerical methods by Zonnerfeld [7].
2	The zeros (dots) and poles (x's) in the upper half complex ϵ -plane of the [48/48] Padé approximant to the amplitude series $A(\epsilon)$ in (3.1). The distance of the singularities from the origin is denoted by R_0 and the angle of the singularity, measured from the positive real axis, is denoted by β_0 . Here $R_0 = 1.85$ and $\beta_0 = 0.8970$.
3	Amplitudes $A(\epsilon)$ computed using the transformed series (4.2) (dotted line), the series (4.4) (dashed line), and the asymptotic formula (4.3) (light dashed line), all expressed as functions of δ given by (4.1). The numerical results of Zonnerfeld [7] are indicated by the heavy dashed line.
4	Phase plane plots for the limit cycle $u(x,t)$ computed using the first 100 terms of the series (2.6) with $\epsilon = 0$ (a), $\epsilon = 1$ (b), $\epsilon = 1.5$ (c), and $\epsilon = 1.6$ (d).
5	The location of the zeros (dots) and poles (x's) in the upper half complex ϵ -plane of the [24/24] Padé approximant to the series (2.6) for $x = \pi/50$ (a), $x = 13\pi/50$ (b), $x = 18\pi/50$ (c), and $x = 24\pi/50$ (d).

Figure

Caption

6

Schematic diagram of the upper half complex ϵ -plane indicating the location of the fixed singularities (*) and the path taken by the moving singularity as x varies between 0 and π . The heavy dotted line indicates a portion of a circle about the origin, of radius R_0 , which corresponds to the radius of convergence of the series (2.6) at $x = 0$.

7

Plots of the distance $R = R(x)$ of the distance of the moving singularity from the origin (a) and the angle $\beta = \beta(x)$ the singularity makes with the positive real axis (b) as functions of x for $0 \leq x \leq \pi$.

8

Phase plane plots of the limit cycle of the Van der Pol oscillator using the transformed series (6.2), with w replaced by w given in (6.3), for $\epsilon = 1.65$ (a) and $\epsilon = 3.5$ (b).

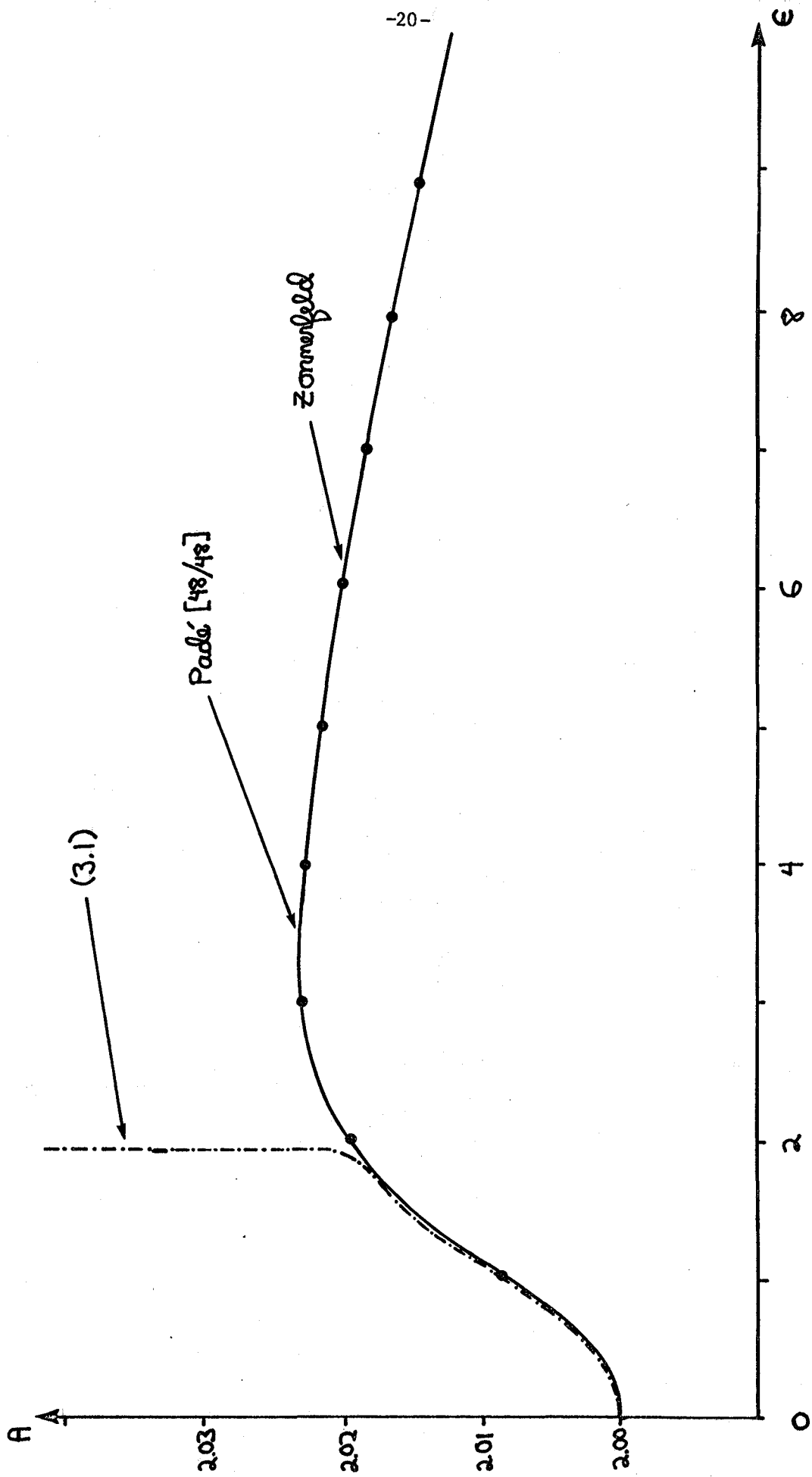


Figure 1

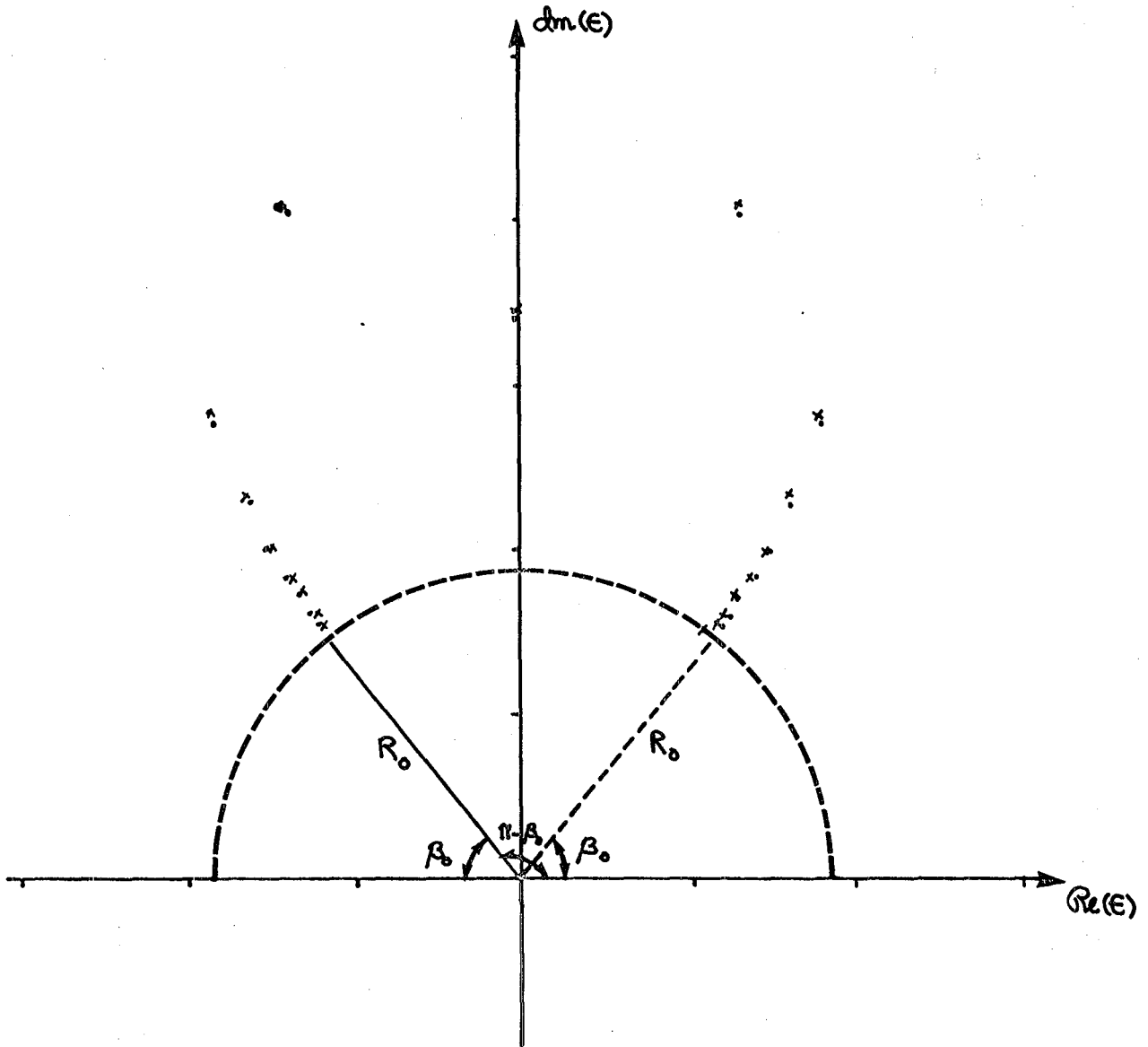


Figure 2

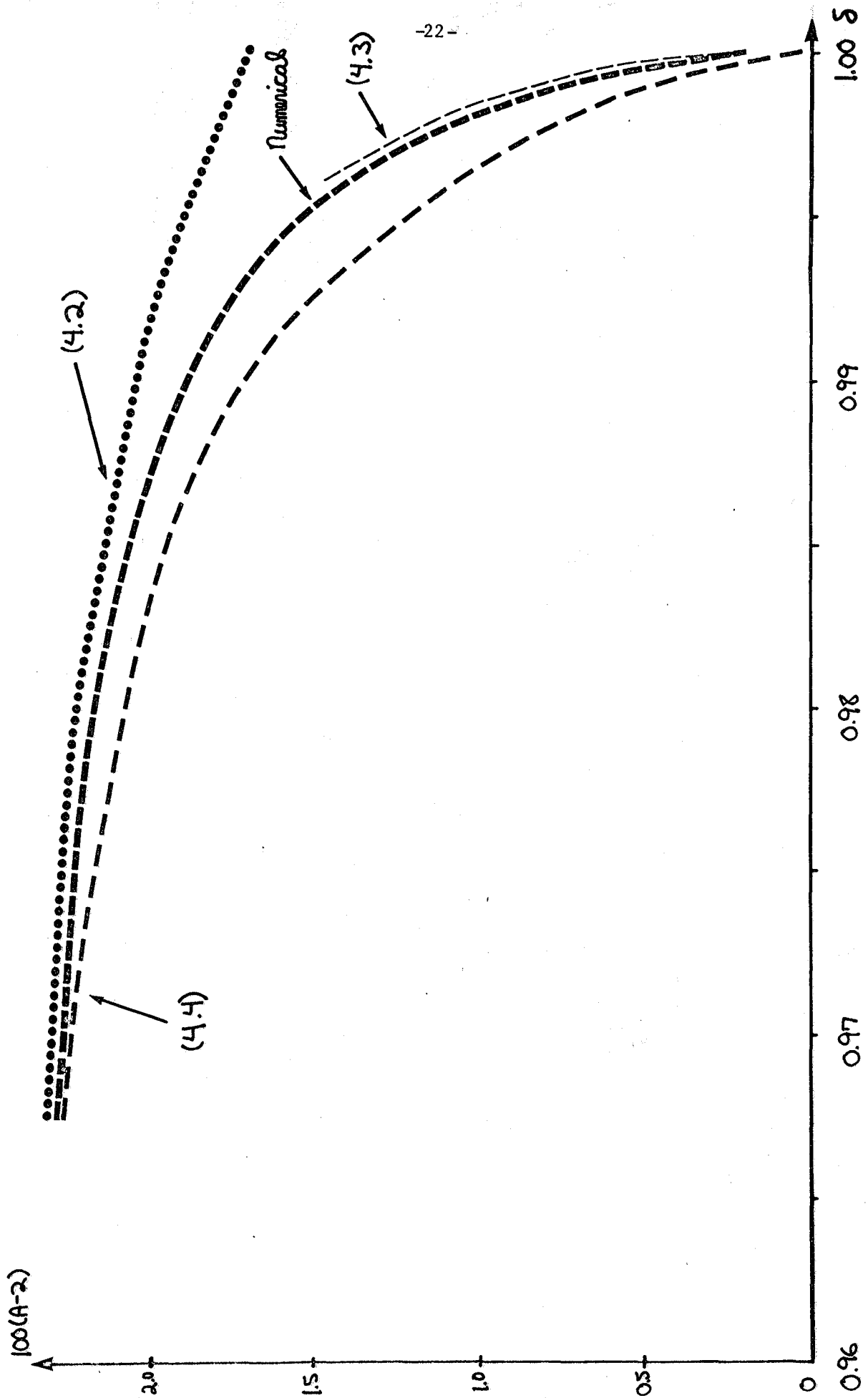


Figure 3

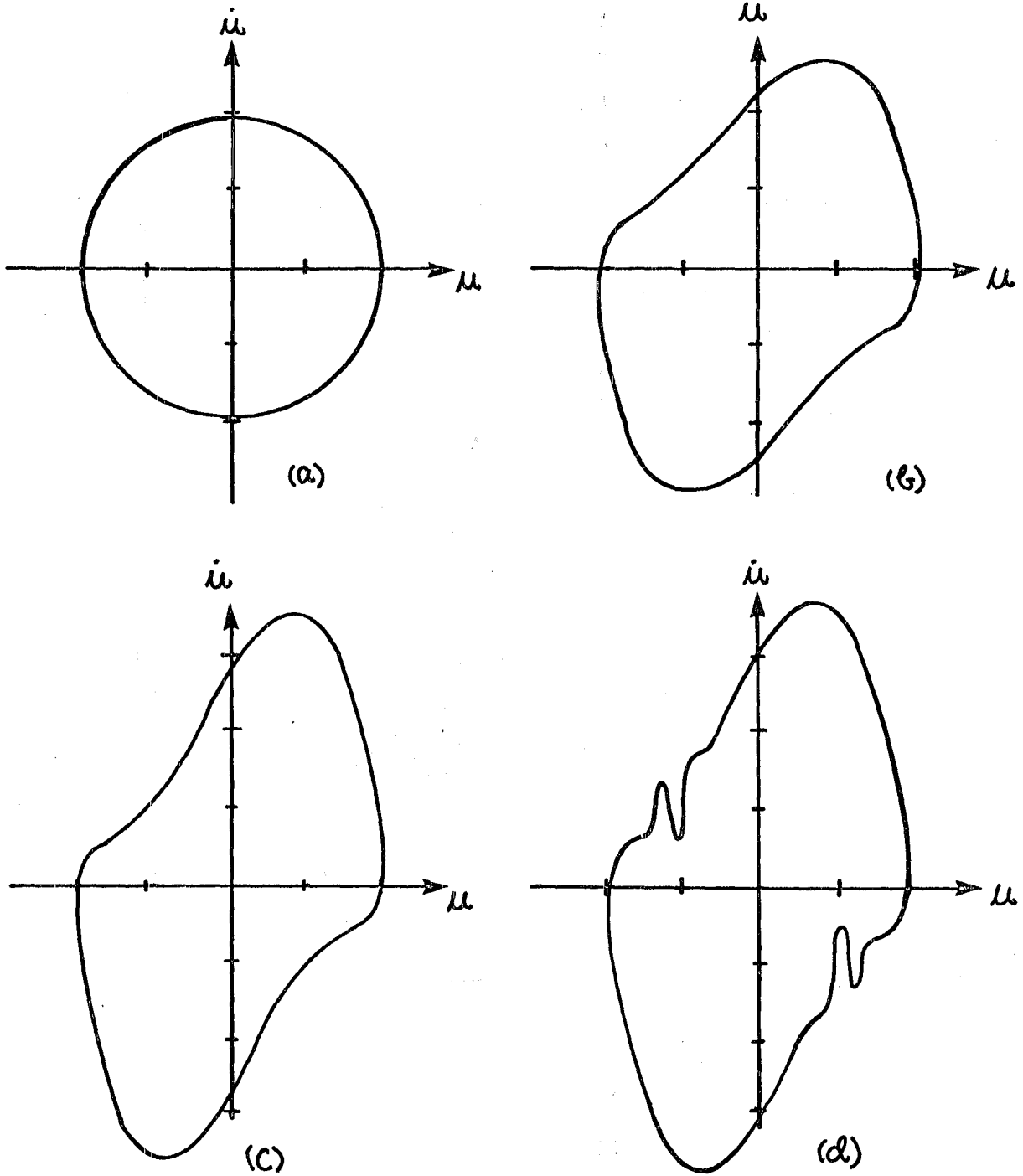


Figure 4

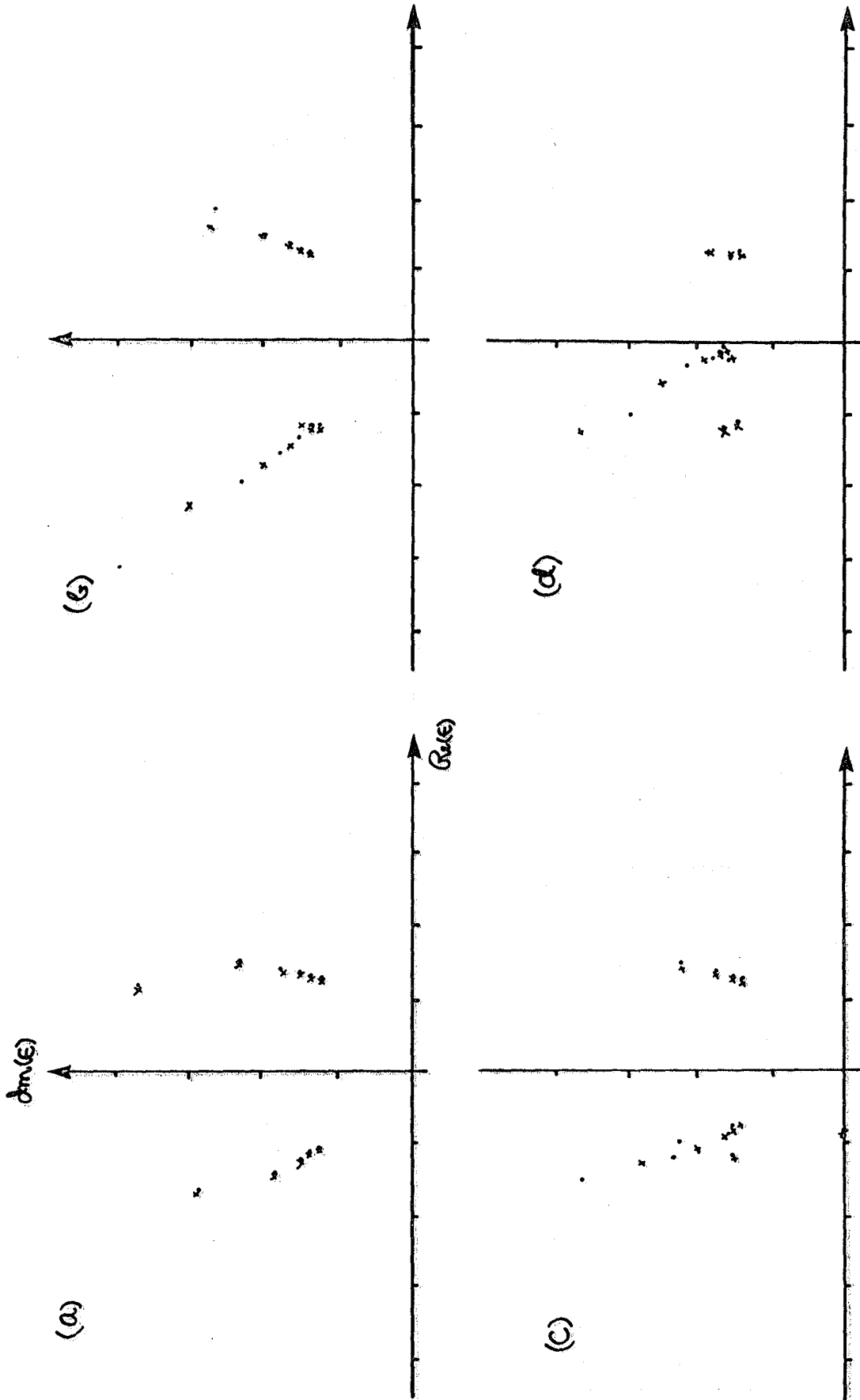


Figure 5

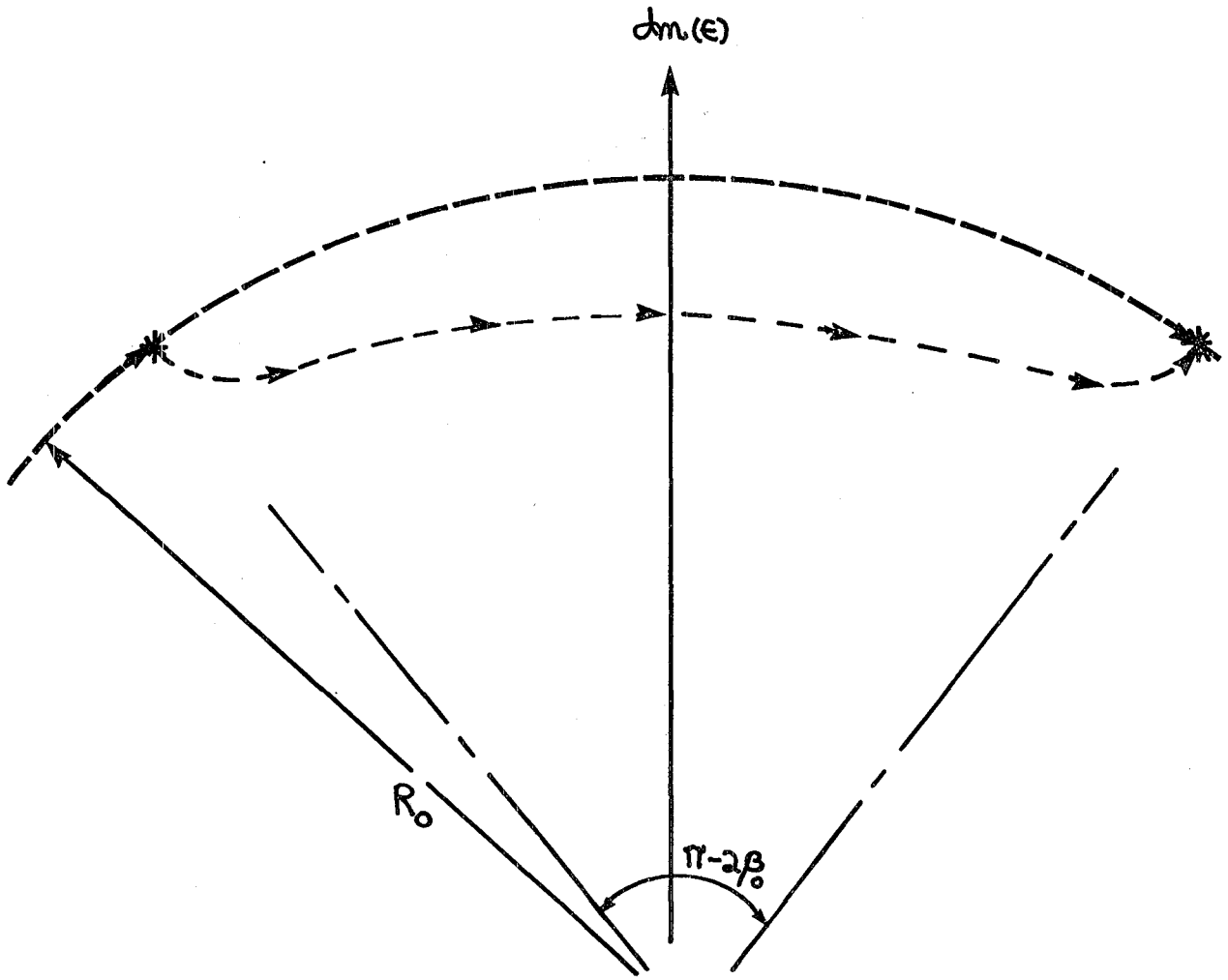


Figure 6

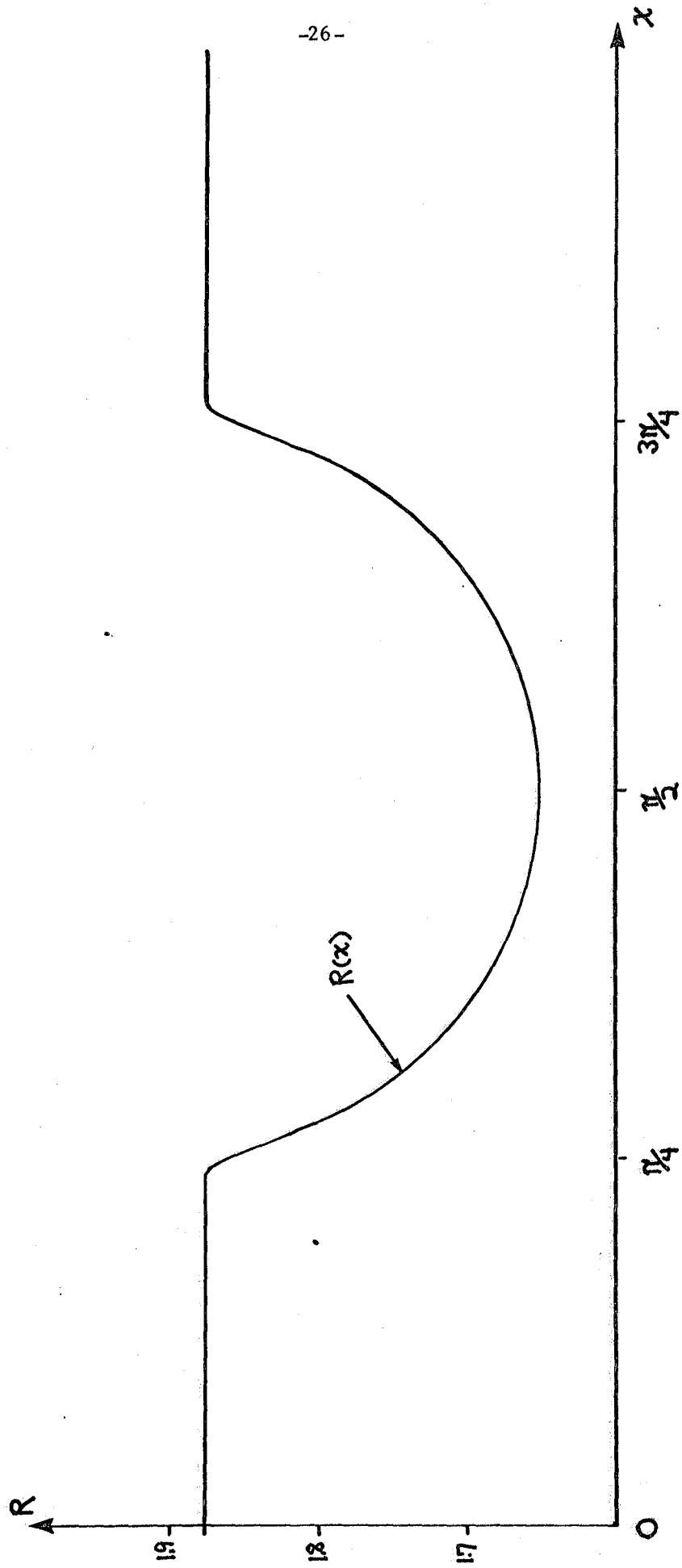


Figure 7(a)

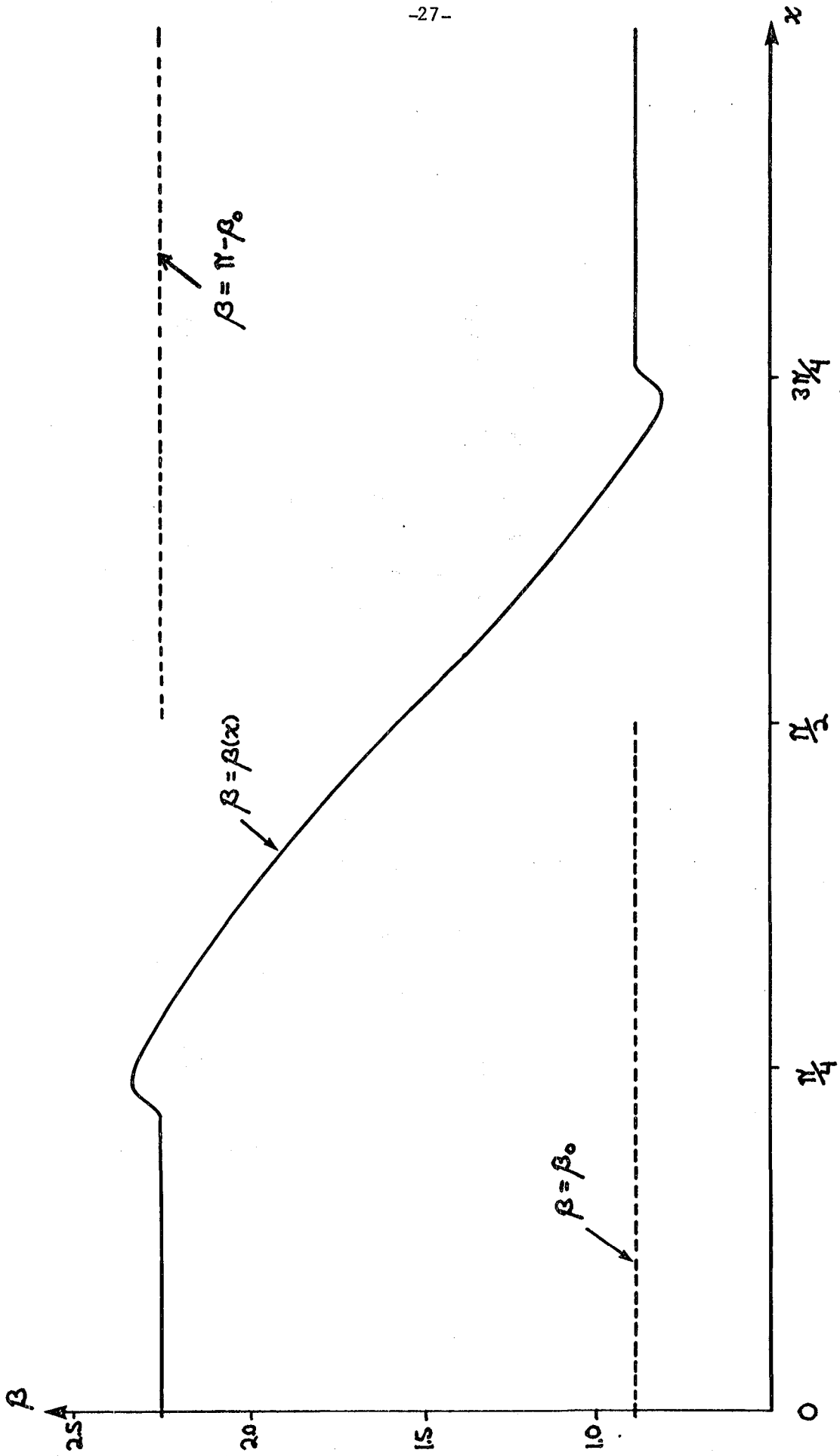
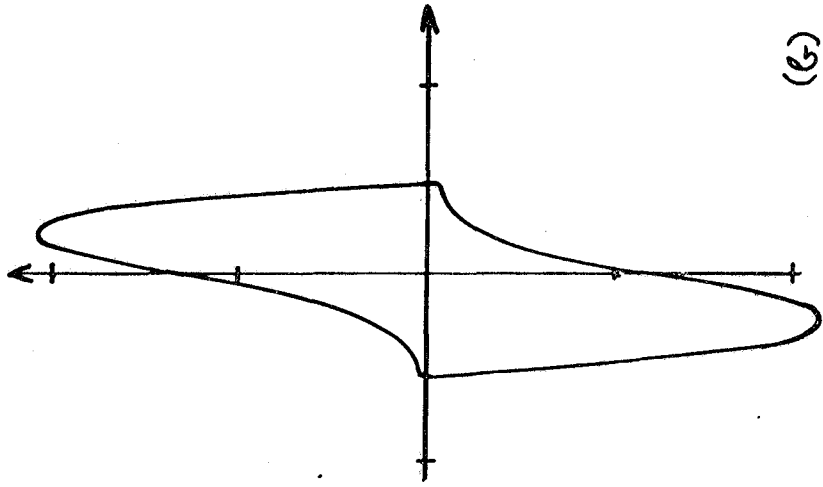
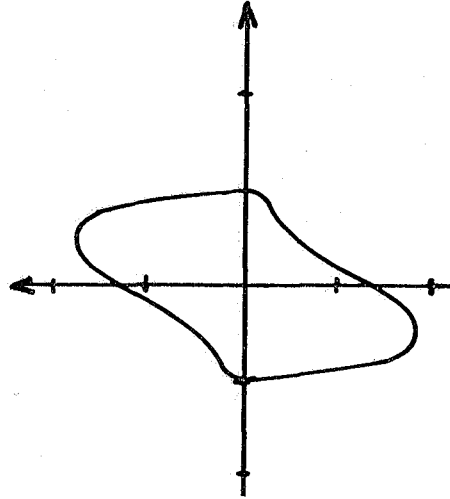


Figure 7(b)



(b)



(a)

Figure 8

- the coefficients a_j

j	a_j
0	.20000000000000000000000000000000D+01
2	.104166666666666666666666666666667D-01
4	-.186812789351851851851851851851850D-02
6	.1829420265767379482657264681D-04
8	.6252074907901755591368089714D-04
10	-.7989632673966515320067624716D-05
12	-.2189064228056858268565719872D-05
14	.6788919544595683082507878164D-06
16	.4898549810605054217263420959D-07
18	-.4647022113222002938983247375D-07
20	.2255473504412209108124923252D-08
22	.2731951082006211951714547135D-08
24	-.4652509830097006092236158866D-09
26	-.1297746287822718370089231457D-09
28	.4708595922064213677321962184D-10
30	.3487493870792913004766338003D-11
32	-.3732111817634004227319748112D-11
34	.1943252115223049791622979950D-12
36	.2450007694080866824617131646D-12
38	-.4352603129565672049761052122D-13
40	-.1280424855985861445787477879D-13
42	.4756220989424199139000255790D-14
44	.3786887176341065017941607400D-15
46	-.4017644262218452857375675723D-15
48	.2019321904821584372579786473D-16
50	.2794375863326511190959233507D-16
52	-.4935965643050148484969066886D-17
54	-.1531839527673392059947190463D-17
56	.5655400842937914902618359951D-18
58	.4870627697603956399462256948D-19
60	-.4964803930073463897595063956D-19
62	.2317473810569203996526550456D-20
64	.3574630974677649035422762246D-20
66	-.6204378348446459588385954659D-21
68	-.2030308157846223288300541515D-21
70	.7366516047524752120471500726D-22
72	.6858589016559903374861711748D-23
74	-.6648782831924194018968477892D-23
76	.2810917947653522342427510213D-24
78	.4910354149106339448267249306D-24
80	-.8312152138347605741759594449D-25
82	-.2867538117024518768030884688D-25
84	.1017007716880446220569768394D-25
86	.1021238904641620465001263825D-26
88	-.9384885053671857224232492601D-27
90	.3512375544271382331382237982D-28
92	.7074331033577236403705433853D-28
94	-.1162685794002263659230791159D-28
96	-.4228793130239495409192460070D-29
98	.1461762114850712338416032999D-29

ϵ	δ	Numerical Amplitudes	amplitudes from (4.2)	amplitudes from (4.4)
1	0.51334687	2.00862	2.00861986 (0.0000)	2.00861986 (0.0000)
2	0.82838459	2.01989	2.01989138 (0.0001)	2.01989138 (0.0001)
3	0.93362980	2.02330	2.02330520 (0.0003)	2.02329950 (0.0000)
4	0.96740216	2.02296	2.02302754 (0.0033)	2.02277836 (0.0090)
5	0.98093575	2.02151	2.02189578 (0.0191)	2.02072554 (0.0388)
6	0.98751267	2.01983	2.02083574 (0.0498)	2.01827716 (0.0769)
7	0.99117650	2.01822	2.02001617 (0.0890)	2.01597957 (0.1110)
8	0.99342421	2.01675	2.01940835 (0.1318)	2.01399777 (0.1365)
9	0.99490355	2.01544	2.01895729 (0.1745)	2.01233709 (0.1540)
10	0.99593011	2.01429	2.01861788 (0.2149)	2.01095469 (0.1656)
11	0.99667240	2.01326	2.01835800 (0.2532)	2.00980079 (0.1718)
12	0.99722702	2.01236	2.01815547 (0.2880)	2.00883125 (0.1754)
13	0.99765264	2.01156	2.01799502 (0.3199)	2.00801004 (0.1765)
14	0.99798658	2.01084	2.01786599 (0.3494)	2.00730865 (0.1756)
15	0.99825355	2.01020	2.01776079 (0.3761)	2.00670472 (0.1739)
16	0.99847042	2.00962	2.01767398 (0.4008)	2.00618069 (0.1711)
17	0.99864904	2.00909	2.01760155 (0.4237)	2.00572273 (0.1676)
18	0.99879794	2.00862	2.01754053 (0.4441)	2.00531985 (0.1643)
19	0.99892340	2.00819	2.01748865 (0.4630)	2.00496326 (0.1607)
20	0.99903011	2.00779	2.01744419 (0.4808)	2.00464585 (0.1566)
30	0.99957293	2.00516	2.01721316 (0.6011)	2.00273757 (0.1208)
40	0.99976056	2.00379	2.01713138 (0.6658)	2.00187300 (0.0957)
50	0.99984699	2.00296	2.01709337 (0.7056)	2.00139359 (0.0782)
60	0.99989383	2.00240	2.01707268 (0.7328)	2.00109396 (0.0652)
70	0.99992204	2.00201	2.01706019 (0.7518)	2.00089125 (0.0559)
80	0.99994033	2.00172	2.01705207 (0.7659)	2.00074619 (0.0486)
90	0.99995286	2.00150	2.01704651 (0.7767)	2.00063792 (0.0431)
100	0.99996183	2.00132	2.01704253 (0.7856)	2.00055442 (0.0383)

Table II

Comparison of the amplitudes computed from equations (4.2) and (4.4) with the numerical amplitudes reported by Zonnerfeld ⁷. The percentage differences are enclosed in parentheses.

ϵ	δ	Asymptotic Amplitudes	amplitudes from (4.2)	amplitudes from (4.4)
10	0.99593011	2.01421561	2.01861788 (0.2186)	2.01095469 (0.1619)
20	0.99903011	2.00783934	2.01744419 (0.4784)	2.00464585 (0.1591)
30	0.99957293	2.00519750	2.01721316 (0.5992)	2.00273757 (0.1227)
40	0.99976056	2.00381131	2.01713138 (0.6647)	2.00187300 (0.0967)
50	0.99984699	2.00297119	2.01709337 (0.7051)	2.00139359 (0.0788)
60	0.99989383	2.00241306	2.01707268 (0.7321)	2.00109396 (0.0659)
70	0.99992204	2.00201806	2.01706019 (0.7513)	2.00089125 (0.0563)
80	0.99994033	2.00172529	2.01705207 (0.7657)	2.00074619 (0.0489)
90	0.99995286	2.00150050	2.01704651 (0.7767)	2.00063792 (0.0431)
100	0.99996183	2.00132306	2.01704253 (0.7855)	2.00055442 (0.0384)
500	0.99999847	2.00017833	2.01702623 (0.8423)	2.00006490 (0.0057)
1000	0.99999962	2.00007301	2.01702572 (0.8476)	2.00002575 (0.0024)
10000	1.00000000	2.00000355	2.01702555 (0.8511)	2.00000120 (0.0001)
INF.	1.00000000	2.00000000	2.01702555 (0.8513)	2.00000000 (0.0)

Table III

Comparison of the amplitudes computed from equations (4.2) and (4.4) with the asymptotic formula (4.3). The percentage differences are enclosed in parentheses.

1. Report No. NASA CR-172166		2. Government Accession No.		3. Recipient's Catalog No.	
4. Title and Subtitle Perturbation Analysis of the Limit Cycle of the Free van der Pol Equation				5. Report Date June 1983	
				6. Performing Organization Code	
7. Author(s) Mohammad B. Dadfar , James Geer, Carl M. Anderson				8. Performing Organization Report No. 83-30	
				10. Work Unit No.	
9. Performing Organization Name and Address Institute for Computer Applications in Science and Engineering Mail Stop 132C/NASA Langley Research Center Hampton, VA 23665				11. Contract or Grant No. NAS1-14101	
				13. Type of Report and Period Covered Contractor report	
12. Sponsoring Agency Name and Address National Aeronautics and Space Administration Washington, DC 20546				14. Sponsoring Agency Code	
15. Supplementary Notes Additional support by U.S. Dept. of Energy Grant ET-78-C-02-4687, Office of Naval Research Grant N00014-77-C-0641 and U.S. Air Force Grant F49620-79-C-020. Langley Technical Monitor: Robert H. Tolson Final Report					
16. Abstract <p>A power series expansion in the damping parameter ϵ of the limit cycle $U(t;\epsilon)$ of the free van der Pol equation $\ddot{U} + \epsilon(U^2 - 1)\dot{U} + U = 0$ is constructed and analyzed. Coefficients in the expansion are computed up to $O(\epsilon^{24})$ in exact rational arithmetic using the symbolic manipulation system MACSYMA and up to $O(\epsilon^{163})$ using a FORTRAN program. The series is analyzed using Padé approximants. The convergence of the series for the maximum amplitude of the limit cycle is limited by two pair of complex conjugate singularities in the complex ϵ-plane. A new expansion parameter is introduced which maps these singularities to infinity and leads to a new expansion for the amplitude which converges for all real values of ϵ. Amplitudes computed from this transformed series agree very well with reported numerical and asymptotic results. For the limit cycle itself, convergence of the series expansion is limited by three pair of complex conjugate branch point singularities. Two pair remain fixed throughout the cycle, and correspond to the singularities found in the maximum amplitude series, while the third pair moves in the ϵ-plane as a function of t from one of the fixed pairs to the other. The limit cycle series is transformed using a new expansion parameter, which leads to a new series that converges for larger values of ϵ.</p>					
17. Key Words (Suggested by Author(s)) Perturbation analysis Nonlinear oscillations Symbolic computation			18. Distribution Statement 59 Mathematical and Computer Sciences (General) Unclassified-Unlimited		
19. Security Classif. (of this report) Unclassified		20. Security Classif. (of this page) Unclassified		21. No. of Pages 32	22. Price A03

End of Document